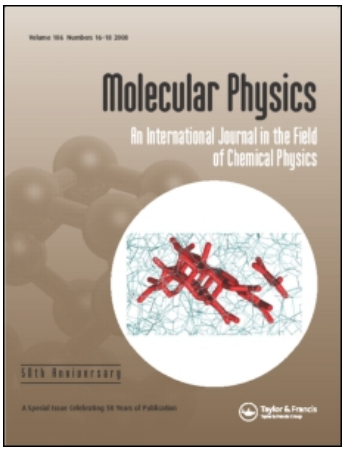

Molecular Physics
Publication details, including instructions for authors and subscription information:
http://www.informaworld.com/smpp/title~content=t713395160

Using molecular dynamic simulation data of calcite in a wide pressure range to calculate some of its thermodynamic properties via some universal equations of state

Hamed Akbarzadeh [a]; Mohammad Shokouhi [a]; Gholam Abbas Parsafar [a]
[a] Department of Chemistry, Sharif University of Technology, Tehran, Iran

Online Publication Date: 01 November 2008

To cite this Article Akbarzadeh, Hamed, Shokouhi, Mohammad and Parsafar, Gholam Abbas(2008)'Using molecular dynamic simulation data of calcite in a wide pressure range to calculate some of its thermodynamic properties via some universal equations of state',Molecular Physics,106:21,2545 — 2556

To link to this Article: DOI: 10.1080/00268970802592379

URL: http://dx.doi.org/10.1080/00268970802592379

Molecular Physics
Vol. 106, Nos. 21–23, 10 November–10 December 2008, 2545–2556

Taylor & Francis
Taylor & Francis Group

RESEARCH ARTICLE

Using molecular dynamic simulation data of calcite in a wide pressure range to calculate some of its thermodynamic properties via some universal equations of state

Hamed Akbarzadeh, Mohammad Shokouhi and Gholam Abbas Parsafar*[1]

Department of Chemistry, Sharif University of Technology, Tehran, 1458881367, Iran

(*Received 3 September 2008; final version received 30 October 2008*)

Molecular dynamics, MD, simulation of calcite ($CaCO_3$) is selected to compare the p-v-T behaviour of some universal equations of state, UEOS, for the temperature range $100\,K \leq T \leq 800\,K$, and pressures up to 3000 kbar. The isothermal sets of p-v-T data generated by simulation were each fitted onto some three- and two-parameter EOSs including Parsafar and Mason (PM), Linear Isotherm Regularity (LIR), Birch-Murnaghan (BM), Shanker, Vinet, Baonza and Modified generalized Lennard–Jones (MGLJ) EOSs. It is found that the MD data satisfactorily fit these UEOS with reasonable precision. Some features for a good UEOS criteria such as temperature dependencies of coefficients, pressure deviation, isothermal bulk modulus and its derivative at the zero pressure limit, isobaric thermal expansion, pressure spinodal values and divergence of pseudo critical exponent either near to or far from the spinodal condition, and some regularities for calcite are investigated.

Keywords: molecular dynamic simulation; calcite; universal equation of state; intermolecular potential; linear isotherm regularity

1. Introduction

Calcite is one of the most common minerals, making up about 4% by weight of the Earth's crust. It is a natural crystal of calcium carbonate, with hexagonal-rhombohedral structure. Calcite fulfils a variety of construction, industrial, agricultural and optical needs. In construction, it makes the primary ingredient of cement. It may also be used as a decorative building stone. In industry, calcite is valuable because it facilitates removal of silica and aluminum impurities of iron, it adjusts pH only enough to reach a non-corrosive equilibrium when it properly applied, and also it may aid in the manufacture of paper and glass. In agriculture, calcite can reduce soil acidity. It has been a popular choice for visible and near-IR polarization optics. It plays a very important role in many scopes across the whole field of the earth science such as order–disorder phase transition at 1260 K [1] and also the use of the isotope fractionation of calcite in geochemistry. A number of microscopic interatomic potential models are reported for calcite in the literature [2].

The purpose of the present work is to generate p-v-T isotherm simulation data of calcite and thereby investigate the precision of some universal EOSs and to calculate some of its thermodynamic properties. Molecular dynamics simulation technique was employed to perform the relevant calculation. Simulations have been performed for different isotherms (100, 200, 300, 400, 500, 600, 700 and 800 K) and pressures up to 3000 kbar.

This paper is organized as follows: Section 2 presents a summary of molecular dynamic trend contained force field model, simulation details and p-v-T simulation results. In Section 3, we summarize some universal equations of state and their merits in predicting the thermodynamic properties of calcite. Then in Section 4, we further check the accuracy of the universal EOSs with the simulation data, and compare their accuracy. Additionally, the temperature dependencies of the parameters of Linear Isotherm Regularity (LIR) II equation of state (EOS) are exclusively examined in Section 5. In Sections 6 and 7, we investigate some regularities in solids and spinodal constraint, respectively. This is followed in the final section by a discussion and conclusion.

2. Molecular dynamic simulation

2.1. *Force field model*

The force field of calcite used in this work is based on the Morse, harmonic and Buckingham force fields. The carbonate anion is handled as a flexible unit with

*Corresponding author. Email: parsafar@sharif.edu
[1]Temporary address: Department of Chemistry, UBC, Vancouver, Canada, V6T 1Z4; email: parsafar@chem.ubc.ca

ISSN 0026–8976 print/ISSN 1362–3028 online

DOI: 10.1080/00268970802592379
http://www.informaworld.com

Morse potential bonds and harmonic bond angles. The Morse potential energy function is of the form

$$u(r) = E_0\left\lfloor(1 - \exp(-K_r(r - r_0)))^2 - 1\right\rfloor, \quad (1)$$

where r is the bond distance of C–O, r_0 is its equilibrium value, E_0 is the well depth (defined relative to the dissociated atoms) and K_r controls the width of the potential well. Intermolecular angle bending motions are described by harmonic functions with force constant K_θ. The potential has the functional form

$$u(\theta) = \frac{K_\theta}{2}(\theta - \theta_0)^2, \quad (2)$$

where θ is the angle between C–O–O and O–C–O; θ_0 is its equilibrium value.

The short-range interactions between Ca–C and Ca–O are treated using simple parameterized equations, such as the Buckingham potential, which takes the form

$$u(r) = A\exp\left(-\frac{r}{\rho}\right) - \frac{C}{r^6}, \quad (3)$$

where $u(r)$ is the potential energy between two atoms and A, ρ, C are parameters particular to the types of atom interacting, with r being the separation between two atoms.

The potential parameters used in this work were first introduced by Pavese *et al.* [3].

Full details of these parameters are tabulated in [4]. The columbic long-range interactions were calculated using Ewald's method, [5–8] with a precision of 1×10^{-6}.

2.2. *Simulation details*

Constant pressure and temperature (NpT) molecular dynamics simulations with 420 molecules were performed using the DLPOLY2.18 [9]. The Verlet-Leapfrog algorithm [10,11] with a time step of 2 fs, was used to integrate the equations of motion; The Nose'–Hoover anisotropic thermostat–barostat with 0.1, 0.1 (ps) relaxation times [12,13] was used to control the temperature and pressure. All interatomic interactions between the atoms in the simulation box and the nearest image sites were taken into account within a cutoff distance of $R_{\text{cutoff}} = 15$ Å for the supercell, which cell vectors are (in angstrom): A(0, 28.78, 0), B(0, 16.78, 29.07), C(29.13, −11.99, −6.92). Partial charges on C, O, and Ca are 1.135, −1.045, 2.

We performed MD calculations for the temperature range 100–800 K at different pressures (0–3000 kbar). The system was equilibrated for 40 ps (20,000 time steps), the averages were computed over the following 400 ps (200,000 time steps).

2.3. *Results of simulation*

We performed NpT simulations of the solid state of calcite to verify the MD procedure and the accuracy of the force field. The experimental [14] and calculated densities for solid calcite at 293 K and 1 bar are respectively, 2.71 and 2.79 g/cm^3. The agreement between the two values is within 2.9%. Simulations were carried out at temperatures ranging from 100 K to 800 K, in 100 K increments, and under the pressure range of 0–3000 kbar. The resulting p-v-T data are given in Table 1.

Table 1. Calculated MD simulation of values at given pressures and temperatures. All data correspond to the volume.

T/K	100	200	300	400	500	600	800
p/kbar	V/(Å)^3						
0	24799	24863	24941	25021	25111	25196	25416
0.01			24940				
1			24906				
10			24604				
200	19988	20045	20105	20163	20185	20231	20362
300	18816	18826	18855	18926	18947	18993	19059
400	17881	17899	17934	17975	18021	18048	18085
500	17134	17159	17207	17230	17231	17259	17326
700	15991		16053	16072	16100	16127	16152
1000	14843	14860	14861	14889	14895	14923	14958
1200	14249	14270	14299	14314	14316	14336	14370
1500	13565	13579	13586	13608	13623	13626	13643
2000	12689	12707	12708	12715	12727	12744	12761
2500	12028	12036	12049	12059	12065	12074	12083
3000	11494	11506	11512	11526	11527	11535	

In Figure 1, we have recorded the radial distribution functions (RDF) of calcite at two temperatures, 100 K and 600 K with $p = 100$ atm. The plots show that as temperature increases, the vibrational motions of the atoms broadens the peaks in the g(r) curves. As temperature rises, the long range correlations are lost and the positions of the maxima, which represent the locations of the neighboring correlation shells, are shifted relative to those of the lower temperature. The results of p-v-T simulation data for each isotherm summarize in Table 1. To obtain the derivative quantities such as bulk modulus B_0 and its isothermal pressure derivative B'_0 for both sets of obtained simulation data, by assuming that there isn't any phase transition in the whole temperature and pressure range in this work, we have fitted p–v data for isotherm 300 K as a reference temperature into the best equation with a high correlation coefficient, $R^2 = 1.000000$, as a best fitting curve and whereby molar density, bulk modulus, B, and its pressure derivation at zero pressure, $(\partial B/\partial p)_T$ when $p \to 0$, are obtained as 27.959 mol/L, 704.080 kbar and 6.057, respectively. It is worth noting that it has been shown that there are two high temperature transitions for calcite at moderate pressures in the temperature range 973–1073 K and around 1273 K [15], which both are beyond the temperatures of this work.

3. Some universal equations of state

The EOSs of solids play an important feature in the condensed matter physics and geophysics. They provide numerous information of non-linear compression of materials at high pressures, and have been widely applied to engineering and other scientific researches. Most EOSs expressed by three zero-pressure parameters: the molar volume, v_0, the isothermal bulk modulus, B_0, and its first isothermal pressure derivative, B'_0. We shall use some well-known universal EOSs below, which have a theoretical base in some extent, to calculate some thermodynamic properties of calcite.

3.1. *Vinet EOS*

One of the most successful isothermal EOSs is that proposed by Vinet *et al.* [16], which is valid for all classes of solids in compression and in the absence of phase transition. The basis of this EOS is a universal relation for the binding energy in terms of the

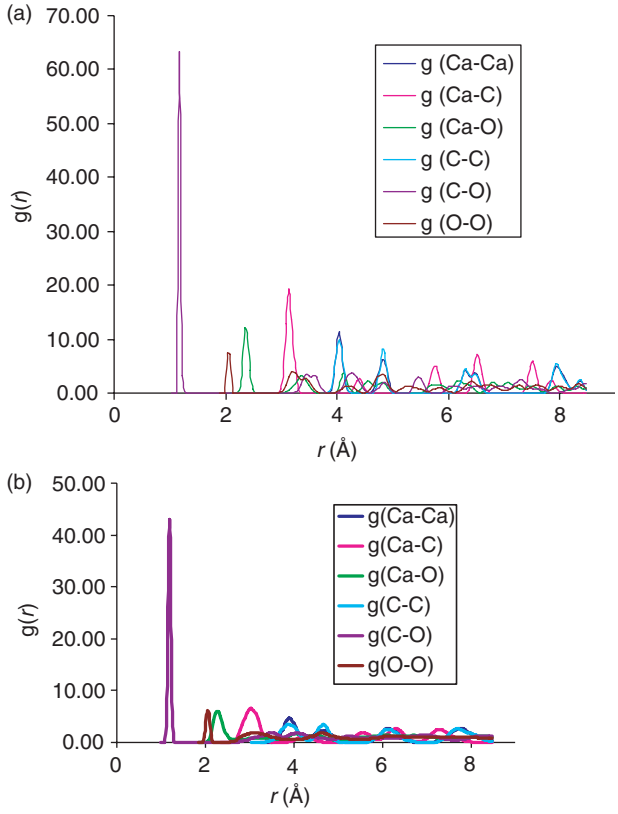

Figure 1. Atom–atom radial distribution functions of calcite at (a) $T = 100$ K; and (b) $T = 600$ K with $p = 100$ atm.

intermolecular distance. In the derivation of this EOS contribution of the thermal pressure is neglected, and the volume derivative of the binding energy is used to approximate the internal energy. Vinet EOS is derived as,

$$p = 3B_0\left[\frac{1-x}{x^2}\right]\exp\left[\left(\frac{3}{2}\right)(B_0'-1)(1-x)\right] \quad (4)$$

in which, $x=(v/v_0)^{1/3}$.

3.2. *Parsafar–Mason (PM) EOS*

Another well-known universal EOS for different solids was presented by Parsafar and Mason [17] only by fitting the repulsive branch of the binding energy curve into a cubic equation in terms of density. The final result is that pv^2 is a quadratic function in density for each isotherm, for which it's scaling parameters, can be related to v_0, B_0 and B_0' in the absence of phase transition:

$$p\left(\frac{v}{v_0}\right)^2 = \left(\frac{1}{2}\right)B_0\left[\left(B_0'-7\right)-2\left(B_0'-6\right)\left(\frac{v}{v_0}\right)+\left(B_0'-5\right)\left(\frac{v}{v_0}\right)^2\right]. \quad (5)$$

3.3. *Birch–Murnaghan (BM) EOS*

In terms of the so-called Birch–Murnaghan EOS [18,19], the pressure as a function of volume behaves as follows:

$$p = \left(\frac{3}{2}\right)B_0\left[\left(\frac{v_0}{v}\right)^{7/3}-\left(\frac{v_0}{v}\right)^{5/3}\right]\times\left\{1-\left(\frac{3}{4}\right)(4-B_0')\left[\left(\frac{v_0}{v}\right)^{2/3}-1\right]\right\}. \quad (6)$$

3.4. *Shanker EOS*

Owing to the fact that the pressure and the isothermal bulk modulus may be expressed as a function of the lattice potential energy, $p=-dU/dv$ and $B=-v(dp/dv)_T=v(d^2U/dv^2)$, and also the derivatives of potential energy with respect to volume may be expressed in terms of the derivatives of U with respect to the intermolecular separation, r, Shanker [20,21] introduced a force constant, A, in terms of Laplacian operator [22], and he found that A may be expressed as a function of volume mentioned in references [20] and [21] then with some mathematical manipulation he obtained the following result known as Shanker EOS,

$$p = \frac{B_0(v/v_0)^{-4/3}}{t}\left[\left(1-\frac{1}{t}+\frac{2}{t^2}\right)\left\{\exp(ty)-1\right\}+y\left(1+y-\frac{2}{t}\right)\exp\left(ty\right)\right] \quad (7)$$

where,

$$y = 1-v/v_0, \quad t = B_0' - 8/3.$$

3.5. *Baonza EOS*

The basis of the Baonza EOS [23] is that the pressure behavior of the isothermal compressibility and thereby bulk modulus of molecular liquid and solid can be characterized by the inverse power law, $B=(1/\kappa^*)(p-p_{SP})^\beta$ in which κ^*, β and p_{SP} are proportionality constant, spinodal exponent and spinodal pressure, respectively. It was found that the value of the exponent β is close to 0.85, the value which will be used here, although Compagner [24] and Speedy [25] have shown that, if the analyticity condition is observed, the value of β should be 1/2, thus this is a shortcoming of Baonza EOS. The integrated equation for the volume which follows proved successful in presenting isothermal data of several liquids and solids,

$$v = v_{SP}\exp\left[-\frac{\kappa^*}{(1-\beta)}(p-p_{SP})^{(1-\beta)}\right], \quad (8)$$

where v_{SP} is the volume where $p=p_{SP}$, which is the maximum volume to which the condenced phase can be expanded and still be metastable. By regarding $p=0$, one may be able to find spinodal parameters, v_{SP} and p_{SP}, in terms of measurable parameters at zero pressure,

$$v_{SP} = v_0\exp\left[\frac{\beta}{B_0'(1-\beta)}\right], \quad (-p_{SP}) = \frac{\beta B_0}{B_0'}, \quad \kappa^* = \frac{(-p_{SP})^\beta}{B_0}. \quad (9)$$

3.6. *Modified generalized Lennard–Jones (MGLJ) EOS*

It is basically arisen from the generalized Lennard–Jones cohesive energy [26] which has also a pivotal

expression in the Gilvarry EOS [27]. One may point out the GLJ EOS as,

$$p = \frac{3B_0}{(m_1 - n_1)}\left[\left(\frac{v_0}{v}\right)^{m_1/3+1} - \left(\frac{v_0}{v}\right)^{n_1/3+1}\right], \qquad (10)$$

which is a two-parameter EOS, and also it is a energy analytic, $U = U(v)$, and pressure analytic, $p = p(v)$, but it is not volume analytic, $v = v(p)$ for arbitrary values of exponents m_1 and n_1. To obtain an EOS for which the energy, pressure and volume are analytic simultaneously, and also it can satisfy the spinodal condition [28], $B \propto (p - p_{SP})^{1/2}$ with $B(p = p_{SP}) = 0$ in which p_{SP} is the spinodal pressure, Jiuxum has considered that the exponents in Equation (10) should satisfy the condition $m_1/3 + 1 = 2(n_1/3 + 1)$ [29]. By substituting the condition in Equation (10), and some algebraic manipulation, he derived the MGLJ EOS as,

$$p = \frac{3B_0}{B_0'}\left[\left(\frac{v_0}{v}\right)^{2B_0'/3} - \left(\frac{v_0}{v}\right)^{B_0'/3}\right]. \qquad (11)$$

3.7. *Linear isotherm regularity (LIR II)*

In a series of works the LIR [30] originally derived for normal dense fluids, was applied to all kinds of fluids [31,32] and also dense fluid mixtures [33,34]. The LIR is able to predict many experimentally known regularities for pure dense fluids and fluid mixtures [35–38]. According to the LIR EOS, $(Z-1)\upsilon^2$ is linear with respect to ρ^2 (where Z is the compressibility factor and $\upsilon = 1/\rho$ is the molar volume) for each isotherm of a fluid, for densities greater than the Boyle density $\rho_B \approx 1.8\rho_C$ and temperatures lower than twice of the Boyle temperature $T_B \approx 2.5$–$2.7T_C$, where ρ_C and T_C are the critical density and temperature, respectively. Recently, we have extended LIR EOS to two classes of solids [39], one for the metallic and ionic solids and the other for the remaining solids on the basis of the concept of the average effective pair potential (AEPP). According to the former EOS, $(Z-1)v^2$ is linear with respect to $1/\rho$ for each isotherm which will be referred to LIR II from now on, and the other EOS is the same as that for dense fluids, i.e. the original LIR.

4. Fitting *p-v-T* simulation data onto universal equations of state

In this section, we apply some UEOSs to calcite to check their abilities in predicting the *p-v-T* behavior or compression data obtained from the MD simulation and to investigate some of its thermodynamic properties. There are two routes to study the compression data, either by using the exact measured values at the zero pressure limit, v_0, B_0, B_0' and B_0'', as inputs in which when the error-free compression and bulk modulus data are available, it can show a perfect well-behaved EOS, or by the curve-fitting trend in which all zero pressure values are obtained as adjustable parameters and can produce the ideal set of zero pressure values. Owing to the fact the zero pressure values obtained by the best fitting haven't high accuracy, both methods for the reference temperature, $T = 300$ K, are applied.

We have fitted all isothermal simulation data of Table 1 into all UEOSs mentioned in the last section. As shown in Figure 2, the simulation data for the reference temperature well fit onto all UEOSs. The values of ρ_0, B_0 and B_0' for 300 K isotherm obtained from the best fitting for each EOS and also from the simulation data accompany with the average percent deviation of pressure are summarized in Table 2. As may be seen from Table 2, PM and MGLJ EOSs show the minimum average pressure deviation, and Shanker EOS shows the maximum deviation. It is worth noting that except for Baonza and LIR II, other EOSs used in this work predict ρ_0 exactly equal to the simulation value.

As the second method, we have used the zero-pressure simulation values as inputs to calculate pressure as function of compression, v/v_0. In Figure 3 pressure is plotted as a function of v/v_0 for calcite at 300 K, and the error curve of pressure for all EOSs are shown in Figure 4, using the zero-pressure simulation values in all EOSs. Although, in the literature [40] it has been shown that Vinet EOS is accurate up to $v/v_0 = 0.3$ for monatomic and diatomic solids, all EOSs used in this work show reasonable results up to $v/v_0 = 0.85$ for calcite, which is a polyatomic salt. However, for high compressions, PM and MGLJ EOSs show quite significant deviations compare to the other EOSs, when the second method is applied. Despite, the fact that LIR II has two parameters; in both methods its prediction is reasonable, in comparison with the other three-parameter EOSs, even with its simplicity. As shown in Figure 4, Dodson EOS [41] has the best agreement with the simulation data.

Using EOS, one can derive an expression for the bulk modulus. With the scaling parameters obtained from the curve-fitting at 300 K, bulk modulus is calculated by using all UEOSs, and its value is plotted as a function of pressure in Figure 5. As may be seen all EOSs show a reasonable behaviour in comparison with simulation data, especially at low and medium pressures.

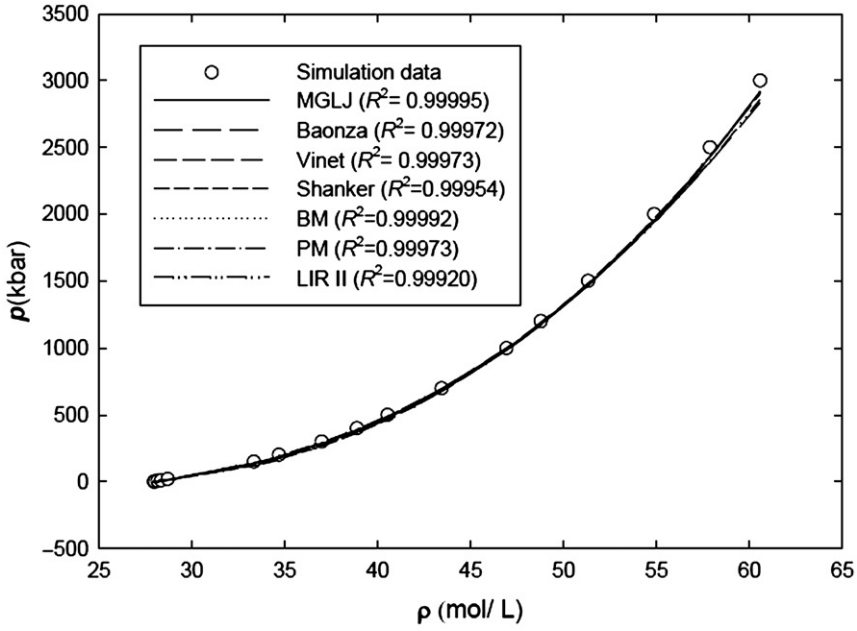

Figure 2. Fitting simulation data of calcite into some universal equations of state at 300 K.

Table 2. Zero pressure quantities of calcite obtained by fitting the simulation data into some UEOSs for reference temperature $T = 300$ K, and average percentage deviation of pressure.

	Simulation	MGLJ	Baonza	Vinet	Shanker	BM	PM	LIR II
ρ_0 (mol/L)	27.959	27.959	28.015	27.959	27.959	27.959	27.959	27.971
B_0 (kbar)	704.080	507.856	503.410	424.811	402.467	491.843	510.147	536.749
B'_0	6.057	5.078	5.250	6.334	6.444	5.305	5.121	5.003
$(\lvert\Delta p\rvert/p)^{a}_{av} \times 100$	...	1.23 (4.87)	1.78 (3.47)	2.92 (11.18)	3.72 (13.83)	1.53 (6.00)	1.17 (4.21)	1.38 (2.50)

[a]The maximum pressure error is given in parentheses.

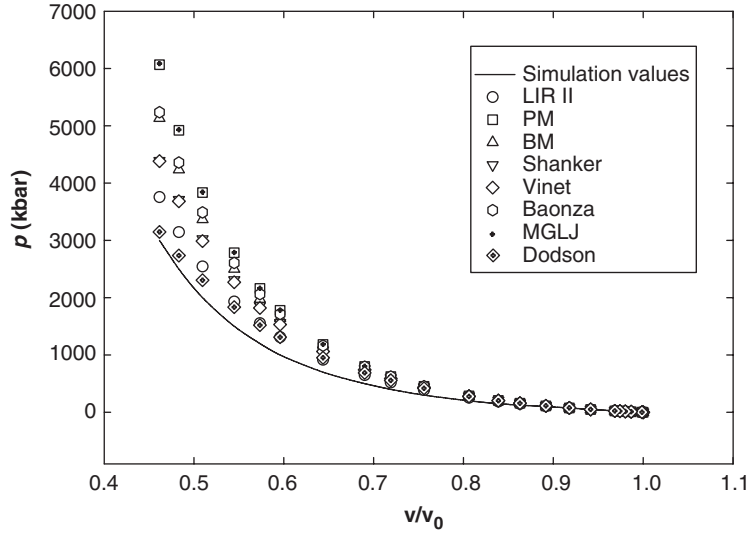

Figure 3. Comparison of the *p-v* isotherm for several EOSs with the zero pressure quantities as inputs.

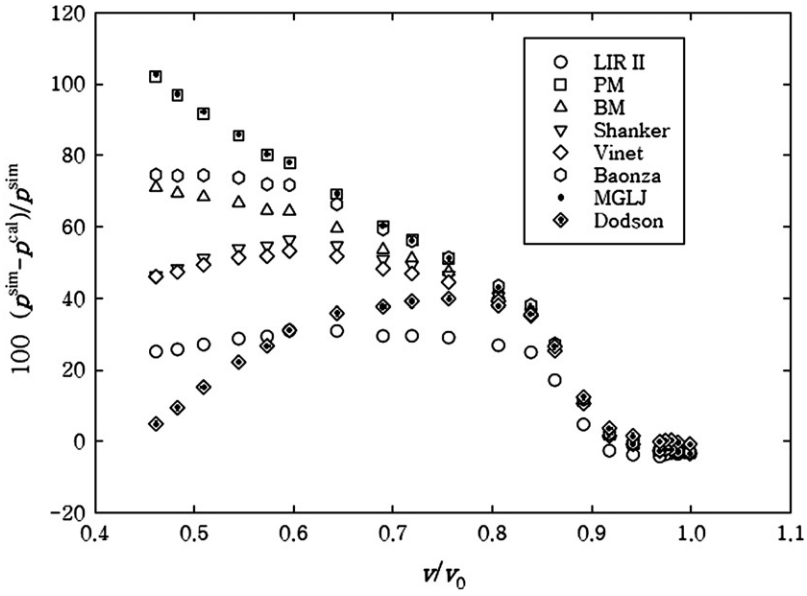

Figure 4. Deviation curve for pressure for some UEOSs in which the zero-pressure simulation values are used as input data.

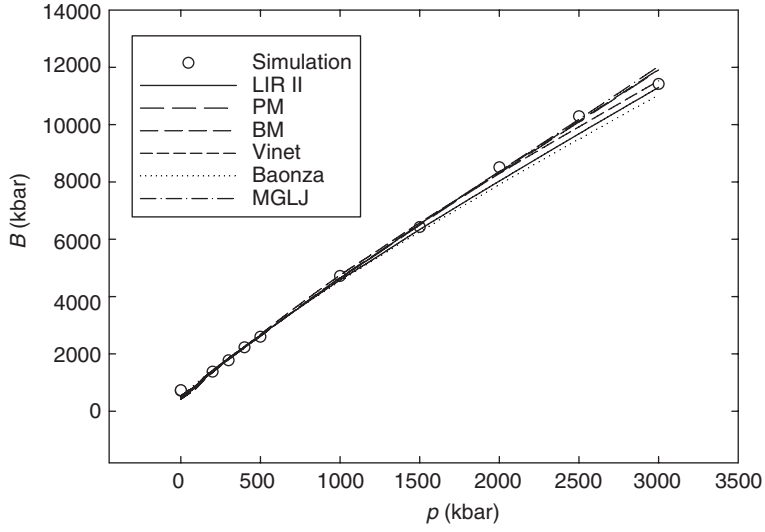

Figure 5. Isothermal bulk modulus for reference isotherm calculated using parameters given in Table 2, and UEOSs which are compared with the simulation data.

5. Temperature dependencies of ρ_0, B_0 and B_0'

The fitting method may be used for other temperatures as well and thereby bulk modulus and its derivative as well as density at the zero pressure as adjustable parameters are obtained which the results are listed in Table 3. As may be seen in Table 3, all EOSs predict that both B_0 and ρ_0 decrease with temperature. At high temperatures the lattice anharmonisity is significant, thereby it will have larger volume and lower density. In a lattice with a larger volume, the average nearest neighbor separation is more, hence its compression at high temperatures is easier, which means it has smaller bulk modulus. Therefore the predictions of the EOSs are reasonable. Based on the values of B_0' in Table 3, all the EOSs predict insignificant change of its value with temperature. Due to the fact that B_0' strictly depends on the exponents of the binding energy, one may expect that they vary with temperature, insignificantly.

Table 3. Zero pressure quantities of calcite obtained by fitting the simulation data into some UEOSs at several temperatures.

T (K)		MGLJ	Baonza	Vinet	Shanker	BM	PM	LIR II
100	B_0 (kbar)	513.364	504.15	429.991	407.703	496.612	515.300	559.197
	B_0'	5.093	5.300	6.347	6.452	5.329	5.136	5.001
	ρ_0 (mol/L)		28.175					28.295
200	B_0 (kbar)	511.980	504.14	427.354	404.339	495.406	514.354	554.853
	B_0'	5.083	5.286	6.346	6.458	5.315	5.126	5.002
	ρ_0 (mol/L)		28.103					28.200
400	B_0 (kbar)	504.174	500.7	421.411	399.051	488.507	507.578	540.600
	B_0'	5.074	5.243	6.332	6.443	5.298	5.113	5.003
	ρ_0 (mol/L)		27.926					27.978
500	B_0 (kbar)	498.779	492.871	416.160	393.624	483.182	501.197	534.492
	B_0'	5.068	5.255	6.332	6.443	5.291	5.113	5.004
	ρ_0 (mol/L)		27.825					27.887
600	B_0 (kbar)	495.466	489.581	413.039	390.401	480.244	497.697	528.206
	B_0'	5.058	5.246	6.324	6.442	5.277	5.106	5.005
	ρ_0 (mol/L)		27.732					27.779
800	B_0 (kbar)	483.305	483.967	410.945	392.553	471.037	486.510	504.453
	B_0'	5.039	5.159	6.227	6.318	5.231	5.085	5.007
	ρ_0 (mol/L)		27.492					27.465

6. Investigation of some regularities using EOS

The purpose of this section is mainly to see how well the simulation data predict some well-known regularities. Although dense systems are usually considered to be complicated on the molecular scale, all of them show some experimentally well-known trends, known as regularities. The Tait–Marnaghan equation is one which has been known for many years. To investigate some regularities predicted by an EOS, the temperature dependencies of its parameters must be known in advance [35,36]. We shall use LIR II because of its simplicity, which may be given as,

$$(Z-1)v^2 = c + d\left(\frac{1}{\rho}\right), \tag{12}$$

where c and d are temperature dependent parameters, as follows:

$$c = c_2 + \frac{c_1}{T} \tag{13}$$

and

$$d = \frac{d_1}{T}, \tag{14}$$

where c_1 and d_1 are related to the attraction and repulsion terms of the average effective pair potential, respectively, while c_2 is related to the non-ideal thermal pressure which it may be regarded as vibrational effect in pressure for solids [39]. Note that pressure has two contributions, the internal pressure which is due to the intermolecular interactions and thermal pressure which is due to the kinetic energy. The parameters c and d may be given in terms of B_0 and ρ_0 as,

$$c = \frac{1}{\rho_0^2}\left(1 + \frac{B_0}{\rho_0 RT}\right), \quad d = \frac{-1}{\rho_0}\left(\frac{B_0}{\rho_0 RT} + 2\right). \tag{15}$$

By the best fitting curve shown in Figure 6 for the solid, the values of c_2, c_1 and d_1 parameters are respectively -0.000487934 ($L^2\,mol^{-2}$), 297.44289 ($L^2\,mol^{-2}\,K^{-1}$) and -8398.5101 ($L\,mol^{-1}\,K^{-1}$) in which the values of coefficient determination for both curves are $R^2 = 1.0000$, show that Equations (13) and (14) have a good accuracy.

Like liquids and supercritical fluids, solids may be usually consider to be complicated on the molecular scale and difficult to predict their properties by thermodynamic method and statistical mechanics due to the complexity and many body interactions among molecules. However, we may expect that solids show a number of simple regularities, like dense fluids, which we wish to investigate such expectation using the simulation data and compare the ability of different UEOSs in predicting these regularities analytically or numerically.

The LIR II EOS may be used to derive analytically the common compression point, ρ_{oz}, as well as the common bulk modulus point, ρ_{OB}, for solids as it was applied to dense fluids. By setting the partial derivative of Z or $(Z-1)v^2$ with respect to temperature equal to zero at $\rho = \rho_{oz}$, we may obtain ρ_{oz} for LIR II as,

$$\rho_{oz} = -\frac{d_1}{c_1} \tag{16}$$

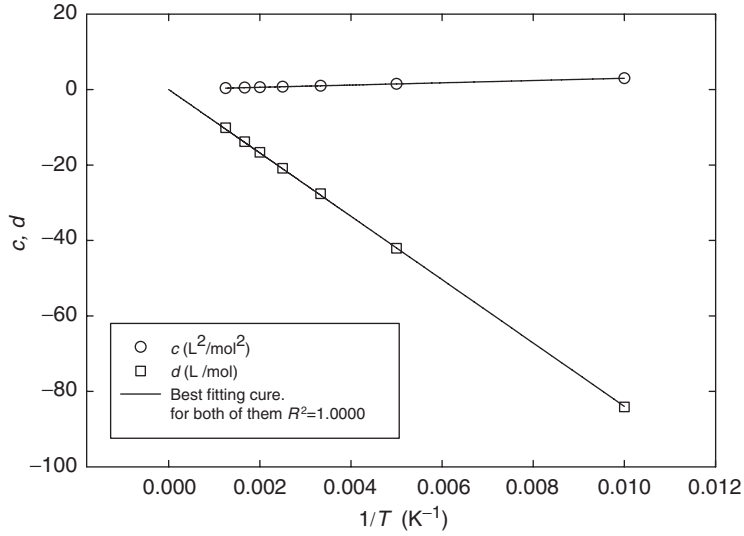

Figure 6. Data of Table 3 for LIR II used to plot the intercept, c, and the slope parameter, d, of Equation (12) for calcite.

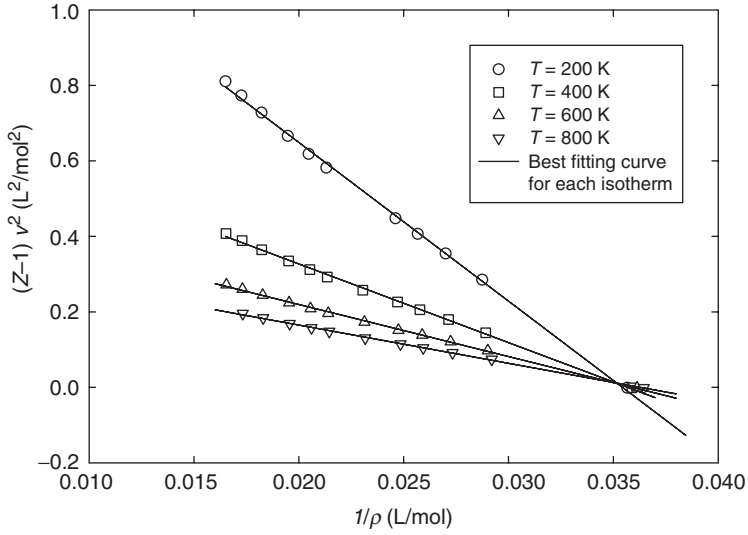

Figure 7. Common intersection point for compressibility factor confirmed by the simulation data and LIR II.

and, on the base of the LIR II, one may show that

$$(B_r - 1)v^2 = 3c + 2d\left(\frac{1}{\rho}\right), \tag{17}$$

where $B_r = B/\rho RT$ is the reduced bulk modulus. In order to find the common bulk modulus point, ρ_{OB}, one may set $(\partial B_r/\partial T)_\rho$ equal to zero to obtain the following result;

$$\rho_{OB} = -\frac{2}{3}\frac{d_1}{c_1} \text{ (from LIR II EOS).} \tag{18}$$

The common intersection point for the compressibility factor is shown in Figure 7. The calculated values of ρ_{oz} and ρ_{OB} for calcite using Equations (16) and (18) are about 28.2 mol/L and 18.8 mol/L, respectively, hence the second value is less than ρ_0 of the isotherms. It is worth noting that the reduced bulk modulus common intersection point is laid a little upper than spinodal density, 18.70 mol/L, which means that under some special condition one may be able to detect it experimentally, simply by having experimental pVT data at relatively low densities. The LIR II EOS may be used to derive the new common intersection point for solids. We have plotted $1/T\alpha_p$ for four different isotherms of calcite, in which α_p is the isobaric expansion coefficient calculated by LIR II, in terms of density which is shown in Figure 8. We can see that

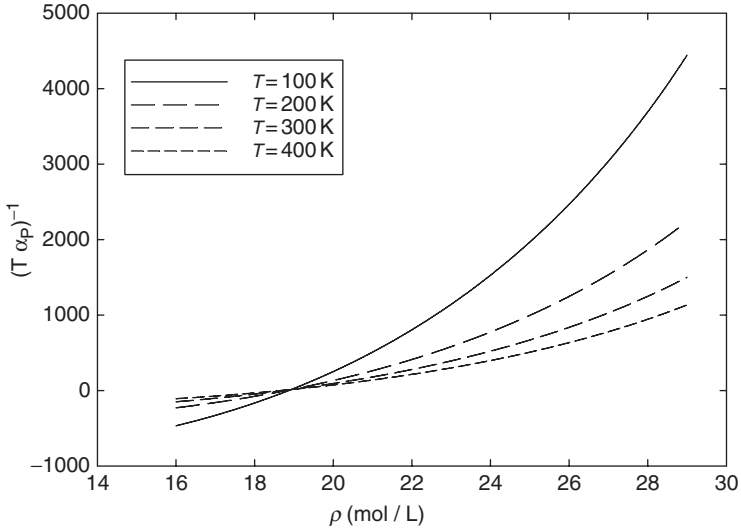

Figure 8. Common intersection point for $1/\alpha_p$ of the isotherms of calcite versus density, which is approximately equal to ρ_{OB}.

all isotherms intersect at $\rho_{\alpha_0} \approx 19$ mol/L which is very close to ρ_{OB}. This may show correlation with some common intersection points of some thermodynamic quantities. To show this claim, we start from correlation between isothermal bulk modulus and isobaric expansion coefficient as,

$$B_r = \frac{(\partial p/\partial T)_\rho}{RT\rho\alpha_P}. \tag{19}$$

Owing to the fact that at the common bulk modulus point, ρ_{OB}, $(\partial B_r/\partial T)_{\rho_{OB}} = 0$, one may use Equation (19) as,

$$\left(\frac{\partial^2 p}{\partial T^2}\right)_{\rho_{OB}} \frac{1}{RT\rho\alpha_p} + \frac{1}{R\rho_{OB}} \left(\frac{\partial p}{\partial T}\right)_{\rho_{OB}} \left[\frac{\partial\left(1/T\alpha_p\right)}{\partial T}\right]_{\rho_{OB}} = 0. \tag{20}$$

By assuming that the thermal pressure of a solid is almost a constant; one may show that the first term in Equation (20) is zero; therefore the common intersection point for isotherms of $1/T\alpha_p$ is approximately the same as that of the bulk modulus.

7. Investigation of spinodal constraint on EOSs using calcite compression data

The spinodal is a locus in the p-v diagram, which is the limit of metastability of a substance with respect to a phase transition. By requiring that the Helmholtz free energy should be analytic at the spinodal, one may be able to derive the limiting behavior of thermodynamic properties near the spinodal by a Taylor series in $V - V_{SP}(T)$, where $V_{SP}(T)$ is the volume of substance close to the spinodal point. The consequence of this analysis is that along an isotherm, close enough to the spinodal,

$$B \propto \alpha^{-1} \propto C_P^{-1} \propto (p - p_{SP}(T))^\beta \tag{21}$$

where C_P is the specific heat. As mentioned before, on the basis of Compagner and Speedy's work [24,25], analytical value of β is 1/2. In order to investigate the value of the exponent not only near the spinodal, one may consider $B = (1/\kappa^*)(p - p_{SP})^\beta$ in the form as

$$\beta = \left(\frac{\partial \ln(B)}{\partial \ln(p - p_{SP})}\right)_T. \tag{22}$$

Substituting $B = -V(dp/dV)$ and $B' = (-V/B)(dB/dV)$ in Equation (19), one may write

$$\beta = \frac{B'}{B}(p - p_{SP}). \tag{23}$$

By using UEOS, the value of β can be calculated from Equation (23) for any density. One may write MGLJ in the following form [29]:

$$B = \frac{2B_0'}{3}\left[(-p_{SP})^{1/2} + (p - p_{SP})^{1/2}\right](p - p_{SP})^{1/2}. \tag{24}$$

As may be seen from Equation (24), MGLJ EOS analytically obeys the spinodal condition irrespective of near or far from the spinodal point, but the Baonza EOS, which is apparently based on the functional form of thermodynamic properties near the spinodal, contradicts the requirement and yields wrong results in the spinodal zone. We have used four different EOSs to calculate β, for which the results are shown in terms of compression in Figure 9. As shown in Figure 9, except

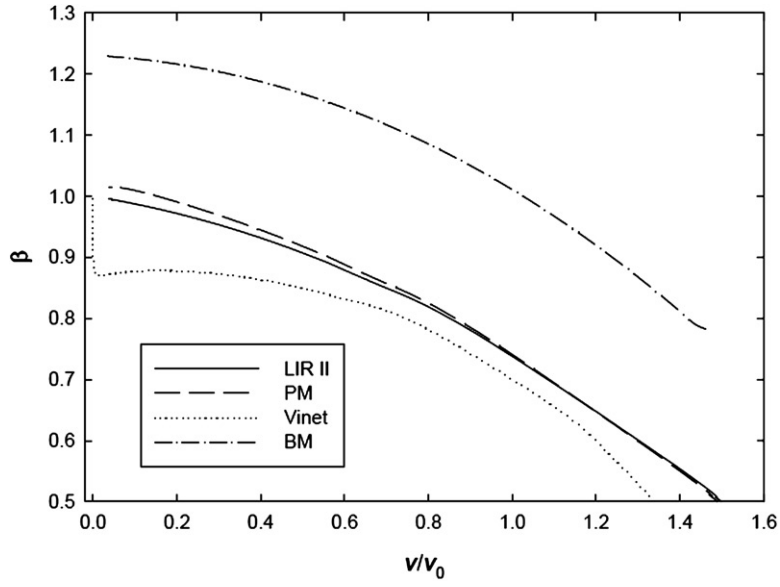

Figure 9. Calculated value of parameter β in terms of compression for LIR II and PM EOSs.

BM which deviates significantly from the spinodal condition for which $\beta(v_{sp}/v_0) \approx 0.79$, all three others, (LIR II, PM and Vinet) obey the spinodal condition as a universal equation of state, since for them $\beta(v_{sp}/v_0) \approx 0.5$. The value of v_{sp}/v_0 for LIR II, PM, Vinet, MGLJ, BM and Baonza are about 1.5, 1.5, 1.34, 1.5, 1.46 and 3.05, respectively, which it is too high for Baonza to be physically reasonable [28,42]. It is worth noting that the value of v_{sp} and β are calculated by spinodal condition, $B \propto (p - p_{SP})^{1/2}$ in which $\beta = 0.5$ and $B(p = p_{SP}) = 0$.

8. Discussion and conclusion

In Table 1, the calculated p-v-T data of calcite obtained by molecular dynamics simulation for pressures up to 3000 kbar are given. We have compared some universal equations of state of solids; namely PM, LIR, BM, Shanker, Vinet, Baonza and MGLJ EOSs; by fitting the simulation data into them and also by using the zero pressure quantities as input data. It is interesting to note that PM gives the most accurate p-v-T presentation when its parameters are considered as adjustable parameters (see Table 2). However, its presentation is very poor especially at high compressions, when the zero-pressure quantities are used as inputs, see Figures 3 and 4. The reason for such a behaviour arises from the fact that PM is based on the fitting only the repulsive branch of the binding energy of solids into a cubic equation in terms of density (see Figures 1 and 2 of [17]), from which one may conclude that higher order of density expansion is needed for the zero pressure limit. Linear isotherm regularity shows very good results in comparison with other EOSs, despite of its simplicity and lower number of parameters. Another merit of LIR is that its adjustable parameters have physical meaning and their temperature dependencies are known. By knowing such temperature dependencies some regularities can be investigated. In Figure 6, we have shown that both LIR II parameters obey the theoretical model, and in Figures 7 and 8, the compressibility factor and bulk modulus intersection points are clearly shown by LIR II. Also, a new regularity has been investigated according to which all isotherms of $1/T\alpha_p$ intersect roughly at a common point which is ρ_{OB}. In Section 7, it is shown that LIR II and PM numerically obey the spinodal condition in which spinodal exponent is 1/2 near the spinodal, which is confirmed by Figure 9. Four different EOSs are used to show the compression dependencies of β in Figure 9, according to which for the medium and high compressions the value of β is reasonable, $0.65 \leq \beta \leq 1$. For Baonza EOS $\beta = 0.85$, which makes it not applicable near the spinodal.

References

[1] M.T. Dove and B.M. Powell, Phys. Chem. Minerals **16**, 503 (1989).
[2] M.T. Dove, B. Winkler, M. Leslie, *et al.*, Am. Mineralogist **77**, 244 (1992).

[3] A. Pavese, M. Catti, S.C. Parker, *et al*., Phys. Chem. Minerals **23**, 89 (1996).
[4] D. Spagnoli, D. Cooke, S. Kerisit, *et al*., J. Mater. Chem. **16**, 1997 (2006).
[5] D. Frenkel and B. Smith, *Understanding Molecular Simulation* (Academic, San Diego, 2000).
[6] M.P. Allen and D.J. Tildesley, *Computer Simulation of Liquids* (Oxford University Press, New York, 1987).
[7] D.C. Rapaport, *The Art of Molecular Dynamics Simulation* (Cambridge University Press, Cambridge, 1995).
[8] K.D. Gibson and H.A. Scheraga, J. Phys. Chem. **99**, 3752 (1995).
[9] W. Smith, T.R. Forester, and I.T. Todorov, *STFC Daresbury Laboratory Daresbury* (Warrington WA4 4AD Cheshire, UK, 2007).
[10] L. Verlet, Phys. Rev. **159**, 98 (1967).
[11] W.F. van Gunsteren and H.J.C. Berendsen, Angew. Chem. Int. Ed. Engl. **29**, 992 (1990).
[12] L.V. Woodcock and K. Singer, Trans. Faraday Soc. **67**, 12 (1971); L.V. Woodcock, J. Chem. Soc. Faraday Trans. II **70**, 1405 (1974); J.W.E. Lewis, K. Singer, and L.V. Woodcock, J. Chem. Soc. Faraday Trans. II **71**, 301 (1975).
[13] S.J. Nose, J. Chem. Phys. **81**, 511 (1984).
[14] O.K. Defoe and H. Compton, Phys. Rev. **25**, 618 (1925).
[15] P.W. Mirwald, Contrib. Mineral. Petrol **59**, 33 (1976).
[16] P. Vinet, J. Ferrante, J.R. Smith, *et al*., J. Phys. C **19**, L467 (1986); P. Vinet, J.R. Smith, J. Ferrante, *et al*., Phys. Rev. B **35**, 1945 (1987).
[17] G.A. Parsafar and E.A. Mason, Phys. Rev. B **49**, 3049 (1994).
[18] F.D. Marnaghan, Proc. Nat. Acad. Sci. USA **30**, 244 (1944).
[19] F. Birch, J. Geophys. Res. **57**, 227 (1952).
[20] J. Shanker, S.S. Kushwah, and P. Kumar, Physica B **239**, 337 (1997).
[21] J. Shanker, S.S. Kushwah, and M.P. Sarma, Physica B **271**, 158 (1999).
[22] M. Born and K. Huang, *Dynamical Theory of Crystal Lattices* (Oxford University Press, Oxford, 1954).
[23] V.G. Baonza, M. Caceres, J. Nunez, Chem. Phys. Lett. **216**, 579 (1993), *ibid* **228**, 137 (1994), V.G. Baonza, M. Caceres, J. Nunez, J. Phys. Chem. **98**, 4955 (1994).
[24] C. Compagner, Physica **72**, 115 (1974).
[25] R.J. Speedy, J. Phys. Chem. **86**, 2002 (1982).
[26] J.X. Sun, H.C. Yang, Q. Wu, *et al*., J. Phy. Chem. Solids **63**, 113 (2002).
[27] J.J. Gilvarry, J. Appl. Phys. **28**, 1253 (1957).
[28] E. Brosh, G. Makov, and R.Z. Shneck, J. Phys.: Condens. Matter **15**, 2991 (2003).
[29] S. Jiuxun, J. Phys.: Condens. Matter **17**, L103 (2005).
[30] G.A. Parsafar and E.A. Mason, J. Phys. Chem. **97**, 9048 (1993).
[31] E. Keshavarzi and G.A. Parsafar, J. Phys. Chem. B **103**, 6584 (1999).
[32] M.H. Ghatee and M. Bahadori, J. Phys. Chem. B **108**, 4141 (2004).
[33] G.A. Parsafar and E.A. Mason, J. Phys. Chem. **98**, 1962 (1994).
[34] G.A. Parsafar and N. Sohrabi, J. Phys. Chem. **100**, 12644 (1996).
[35] B. Najafi, G.A. Parsafar, and S. Alavi, J. Phys. Chem. **99**, 9248 (1995).
[36] S. Alavi, G.A. Parsafar, and B. Najafi, Int. J. Thermophys. **16**, 1421 (1995).
[37] V. Moieni, J. Phys. Chem. B **110**, 3271 (2006).
[38] J. Tian and Y. Gui, J. Phys. Chem. B **111**, 1721 (2007).
[39] M. Shokouhi, G.A. Parsafar, and M.H. Dinpajooh, Fluid Phase Equilibria **271**, 94 (2008).
[40] J. Hama and K. Suito, J. Phys.: Condens. Matter **8**, 67 (1996).
[41] B.W. Dodson, Phys. Rev. B **35**, 2619 (1987).
[42] R.G. McQueen and S.P. Marsh, J. Appl. Phys. **33**, 654 (1962).